Polychromatic Optical Vortex Generation from Patterned Cholesteric Liquid Crystals

Junji Kobashi,[1] Hiroyuki Yoshida,[1,2,*] and Masanori Ozaki[1]
[1]Division of Electrical, Electronic and Information Engineering, Graduate School of Engineering, Osaka University, 2-1 Yamada-oka, Suita, Osaka 565-0871, Japan
[2]Japan Science and Technology Agency, Precursory Research for Embryonic Science and Technology (JST PRESTO), 4-1-8 Honcho, Kawaguchi, Saitama 332-0012, Japan
(Received 5 April 2016; published 22 June 2016)

Generation of optical vortices is described in cholesteric liquid crystals with a singular point in the spatial distribution of a helix phase. The phenomenon uses the fact that a Bragg reflected light phase varies in proportion to the spatial phase of the helix, both at normal and oblique incidences. Our proposal enables high-efficiency, polychromatic generation of optical vortices without the need of a cumbersome fabrication process and fine-tuning.

DOI: 10.1103/PhysRevLett.116.253903

Optical vortices are screw wave front dislocations in an optical field around which the phase is twisted by $2\pi\ell$, where ℓ is an integral number called the topological charge of the singularity [1,2]. They carry orbital angular momentum of light that is separate from the spin angular momentum of light, which corresponds to the polarization. Optical vortices have attracted attention since the early 1990s because of their properties such as structurally stable propagation, circulatory energy flow around the axis, and zero intensity along the on axis. They are also attractive from the point of view of applications, as they enable rotational control of microsized objects, quantum communication, coronagraph, and edge enhancement in microscopy [3–7].

To date, various methods have been proposed for the generation of optical vortices, such as spiral phase plates, holographic elements, liquid crystal q plates and droplets, and metasurfaces [8–16]. However, most devices operate at a single wavelength, and require precise fabrication or tuning to maximize the conversion efficiency. Some diffractive components can operate at multiple wavelengths; however, an additional prism or spatial phase modulator is required to compensate the dispersion [17]. A facile and robust means to generate optical vortices is of great utility for various applications.

Here, we describe the polychromatic generation of optical vortices via reflection off a cholesteric liquid crystal (ChLC): a one-dimensional photonic structure with a helical dielectric tensor variation. They exhibit Bragg reflection over wavelengths $n_o p$ and $n_e p$, where n_o, n_e, and p are the ordinary and extraordinary refractive indices and pitch, respectively. Interestingly, the reflected light phase is directly proportional to the spatial phase of the helix; therefore, an optical vortex beam can be generated by creating a distribution of the spatial phase of the helix such that it contains a singular point around which the phase varies by integral multiples of π. Because the device operates on Bragg reflection, it is polychromatic and does not require tuning to maximize the conversion efficiency. Moreover, by exploiting the angular dependence of the Bragg reflection band, quasi-polarization-insensitive vortex generation can be achieved at oblique incidence.

We first derive an approximate solution for the phase of light reflected off a ChLC with arbitrary spatial phase. Consider a right-handed ChLC with the helix axis along the z direction. The angle between the long axis of the local director and the x axis is set to φ at $z = 0$. For light propagating along the z axis, the dielectric tensor can be reduced to a 2×2 dielectric matrix, given by

$$\boldsymbol{\varepsilon}(z) = \bar{\boldsymbol{\varepsilon}} + \Delta\boldsymbol{\varepsilon}(z) = \bar{\varepsilon}\begin{pmatrix} 1 & 0 \\ 0 & 1 \end{pmatrix} + \frac{(n_e^2 - n_o^2)}{2}\begin{pmatrix} \cos 2\Phi(z) & \sin 2\Phi(z) \\ \sin 2\Phi(z) & -\cos 2\Phi(z) \end{pmatrix}, \quad (1)$$

where the first and second terms represent nonperturbative and perturbative terms, $\bar{\varepsilon} = (n_e^2 + n_o^2)/2$, $\Phi(z) = qz + \varphi$, $q = 2\pi/p$. According to the coupled-mode theory for media with periodic perturbations, the reflection coefficient of ChLC can be expressed as [18,19]

$$r = \frac{-i\kappa^* \sinh sL}{s\cosh sL + i(\Delta k/2)\sinh sL}, \quad (2)$$

where κ is the coupling coefficient, s is given by $s^2 = \kappa\kappa^* - (\Delta k/2)^2$, $\Delta k = 2k - 2q$, $k = 2\pi\varepsilon^{1/2}/\lambda$ is a wave vector inside the helix, λ is the wavelength, and L is the length of the helix. The coupling coefficient for a right-handed circular polarized (RCP) light is given by

$$\kappa = \frac{\omega^2\varepsilon_0\mu_0}{2k}\boldsymbol{E}_1^*\Delta\boldsymbol{\varepsilon}\boldsymbol{E}_2 = \frac{\pi(n_e^2 - n_o^2)}{2\lambda\sqrt{\bar{\varepsilon}}}\exp(2i\varphi), \quad (3)$$

where the normalized forward and backward going RCP light is described by the Jones electric-field vectors $E_1 = E_0 \times [1, i]^{\mathrm{T}}$ and $E_2 = E_0 \times [1, -i]^{\mathrm{T}}$. The reflected phase Φ_r is the argument of the reflection coefficient,

$$\Phi_r = \arg(r) = -\frac{\pi}{2} - 2\varphi - \tan^{-1}\frac{s\cosh sL}{(\Delta k/2)\sinh sL}. \quad (4)$$

From Eq. (4), Φ_r depends on twice the value of φ [20]. The phase change is independent of the wavelength when Bragg's law is satisfied ($\Delta k \approx 0$); therefore, the geometrical phase effect is polychromatic, operating over the wavelength region $n_o p - n_e p$.

The operation wavelength can be controlled from far infrared to ultraviolet simply by changing the pitch of the ChLC. Also, because liquid crystals are dielectric, losses only become problematic at short ultraviolet wavelengths where molecular absorption occurs. This is an advantage over other optical vortex generators such as metallic or dielectric metasurfaces [15,16], which suffer from losses in the visible range, and nematic liquid crystal q plates [12], which show a high conversion efficiency only at limited wavelengths.

Vortex generation based on the above concept is experimentally demonstrated using a right-handed ChLC material prepared from a nematic liquid crystal (Merck, BL-006) and a chiral dopant (Merck, CD-X) mixed at a weight ratio of 96.3:3.7. The material exhibited a reflection band between 580 and 680 nm. A 9-μm-thick glass sandwich cell was prepared from two glass substrates coated with a photoaligning layer (DIC, LIA-03) that sets its orientational easy axis perpendicular to the incident polarization [21]. The cell was photopatterned using a polarizing projection exposure system to have an easy axis distribution, $\varphi(x, y)$, at the surface of the substrate. The pattern was described by $\varphi(x, y) = s\psi + \varphi_0$, where s is called the strength of the singular point and is an integer or a half-integer, $\psi = \tan^{-1}(y/x)$, and φ_0 is the orientation angle on the x axis. The pattern has a singular point at the origin and generates an optical vortex with topological charge $\ell = 2s$ due to Eq. (4). Figure 1(a) shows $\varphi(x, y)$ for $s = 1/2$ and 1 with $\varphi_0 = 0$. After cell patterning, the ChLC was injected into the cell in the isotropic phase and then cooled to room temperature to set its helix axis along the cell normal direction. Under an ordinary polarizing microscope, the samples appear uniform as shown in Fig. 1(b); however, fork-shaped fringes characteristic of optical vortices are observed when viewed with a microscopic white-light Michelson interferometer [Fig. 1(c)] (setup is described in Ref. [20]). Insertion of band-pass filters with center wavelengths falling within the reflection band (580 and 633 nm) confirms the polychromatic nature of optical vortex generation. As shown in Fig. 1(d), the experimental interferograms are numerically reproduced by calculating

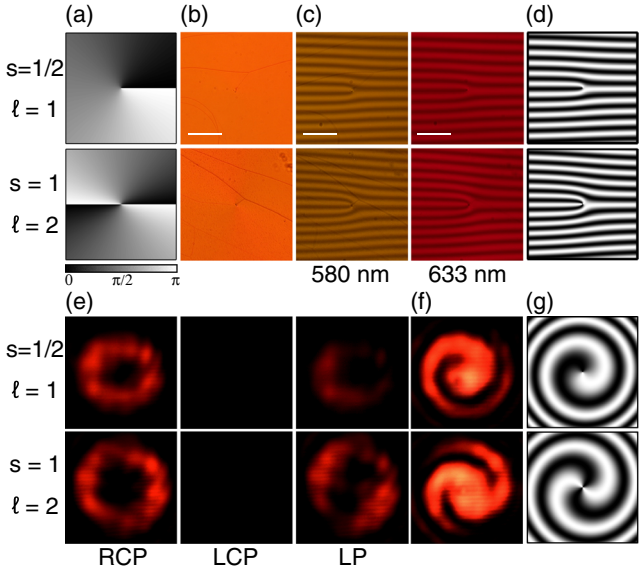

FIG. 1. Device design and experimental photographs of patterned cholesteric liquid crystals (ChLCs) with topological charge $\ell = 1$ and 2. (a) Spatial phase distribution of ChLC at the surface of substrate. (b) Polarized micrographs. Scale bar: 200 μm. (c) Measured and (d) simulated interferograms of the phase of reflected light. Scale bar: 200 μm. (e) Light spot detected by a camera at normal incidence of right and left-handed circularly (RCP, LCP), and linearly polarized (LP) light without reference beam. (f) Measured and (g) simulated light spot with reference beam at RCP light incidence.

the interference of a beam having a phase distribution of $2\varphi(x, y)$ and a tilted plane wave [22].

Optical vortex generation was also confirmed by directly observing the reflected light spot of a laser. A He-Ne laser (633 nm) was spatially filtered by passing it through a single-mode fiber and collimating lens, and was incident normally on the sample, after being reflected by a non-polarizing cube beam splitter. The profile of the reflected beam was observed on a CCD camera after passing it through the beam splitter. An optical isolator composed of a polarizer and a quarter-wave plate was placed between the beam splitter and the sample to control the incident polarization as well as block light reflected from the surface of cell (light reflected from the ChLC is not eliminated as the polarization handedness does not change). The wave front of the laser beam was visualized by placing a lens and an aluminum mirror in the transmitted path of the incident beam, to form a Michelson interferometer.

Figures 1(e) and 1(f) show the light spot reflected off the cell with and without the reference beam. For RCP light incidence, a doughnutlike intensity profile is observed, which increases its inner radius with an increase in topological charge [Fig. 1(e), left]. For the left-handed circularly polarized (LCP) light incidence, no reflection is observed [Fig. 1(e), center] and, for the linearly polarized (LP) light incidence, a dim doughnutlike pattern is observed [Fig. 1(e), right]. With the spherical reference

beam superposed, an anticlockwise outgoing branched spiral is observed, with the number of branches varying as ℓ [Fig. 1(f)]. The profile is reproduced numerically by assuming the superposition of an optical vortex with positive topological charge with a spherical wave front [Fig. 1(g)]. The results again prove optical vortex generation, and moreover, demonstrate the near-perfect circular polarization selectivity of the phenomenon.

Because device operation is based on the control of Bragg reflected light phase, the theoretical conversion efficiency depends on the reflectivity of the ChLC. This means that theoretically, 100% efficiency is achieved for normally incident light falling within the wavelength range $n_o p - n_e p$ with the same circular polarization handedness as the helix. In conventional diffractive devices optimized for use under normal incidence, the conversion efficiency decreases as the incidence angle increases. In the case of ChLC for oblique incidence, the reflection band blueshifts and the circular polarization selectivity is lost, leading to a lowered conversion efficiency. However, for sufficiently large incident angles, a reflection band appears for both circular polarizations [23]. The phase of light reflected by the "total" reflection band also depends on the spatial phase, and can be exploited to generate optical vortices irrespective of the incident polarization, resulting in enhanced conversion efficiency.

Figures 2(a) and 2(b) show the incident angle dependence of the reflectance of a ChLC calculated by Berreman's 4×4 matrix method [24]. A ChLC with refractive indices $n_e = 1.78$, $n_o = 1.53$, and helical pitch $p = 360$ nm was assumed to exist between two glass substrates separated by 9 μm ($n_{\text{glass}} = 1.53$). These parameters were chosen as they are close to the experimental values. Taking the helical axis along the z axis, the ChLC was assumed to have its local director along the x axis at $z = 0$ and 9 μm, and the incident angle was varied in the z-x plane. For RCP light incidence, the reflection band blueshifts from ≈600 nm at normal incidence to ≈300 nm at 60° with a near cosine dependence [Fig. 2(a)]. The reflectivity within the reflection band gradually becomes nonuniform, with two regions of low reflectivity appearing around a narrow central band with almost 100% reflectivity. For LCP light incidence, no reflection is observed up to about 22°, but a narrow reflectance band appears for greater incidence angles, and gradually grows in reflectance.

Figures 2(c) and 2(d) show the spatial helix phase dependence of the reflected light phase at the center wavelength of the reflection band [calculated along the dashed line in Figs. 2(a) and 2(b)]. For each angle of incidence, the reflected light phase was normalized to the value at 0 spatial phase. For RCP incidence, the reflected phase is approximately proportional to the spatial phase of the helix, regardless of the incident angle [Fig. 2(c)]. A similar relationship is also found for LCP light when the reflectance is sufficiently high (above approximately 30°); however, the relationship deviates from a linear relationship at shallow incident angles and, below 22° where there is negligible reflection, the variation in reflected phase reduces to below π.

Incident-polarization-insensitive optical vortex generation was verified experimentally using the same material as that for normal incidence. Considering the availability of

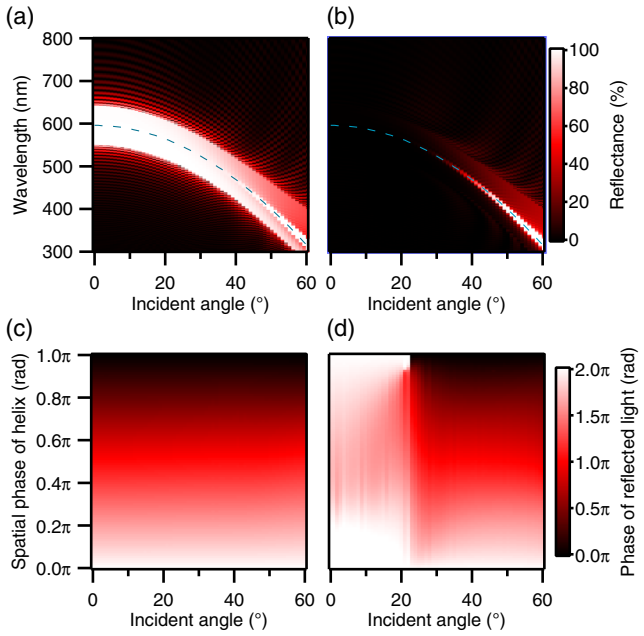

FIG. 2. Optical properties of ChLC at various incident angles. Reflectance for RCP (a) and LCP incident light (b). Phase of reflected light at the center wavelength (blue dashed line) of the reflection band for RCP (c) and LCP incident light (d).

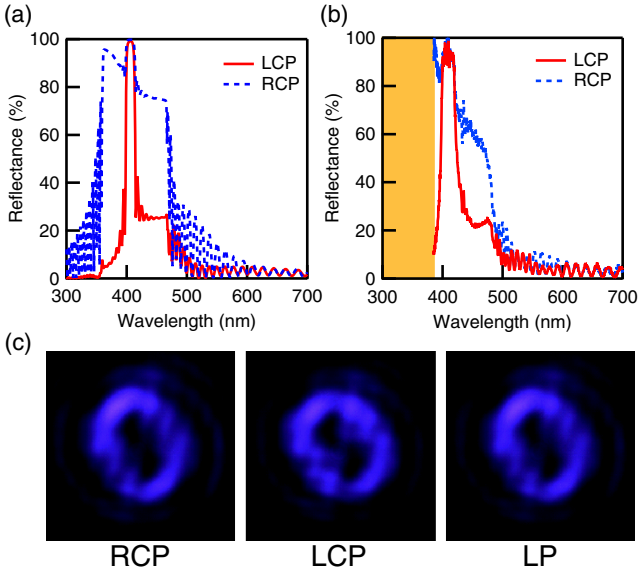

FIG. 3. Calculated (a) and measured (b) reflectance of the ChLC cell upon oblique incidence at 49°. (c) Measured reflected light spot of a violet laser ($\lambda = 405$ nm) for RCP, LCP, and LP light.

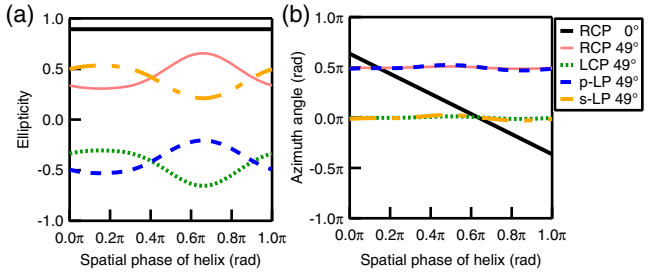

FIG. 4. Polarization state of the light reflected off from ChLC at various spatial phases of the helix for RCP, LCP, $p(s)$-polarized LP (p-LP, s-LP) light. (a) Ellipticity (left-handedness of circular polarization is shown by negative). (b) Azimuth angle.

laser wavelengths, the incident angle was set to 49° to obtain reflection around 405 nm. Figures 3(a) and 3(b) plot the calculated and experimental reflectance at 49° incidence, measured by placing a right-angled prism made of BK-7 on the sample. The results are in good agreement, with a total reflection band of bandwidth approximately 20 nm appearing around 410 nm. Figure 3(c) shows the light spot of a semiconductor laser with a wavelength of 405 nm reflected off the device with a spatial phase distribution of $s = 1$. A modified pattern defined by $\varphi = s\tan^{-1}\{y/[x\cos(49 \times \pi/180)]\}$ was used to compensate for the device tilt. It is seen that RCP, LCP, and linearly polarized (LP) light (polarized along the y axis) are converted into an optical vortex with a doughnutlike intensity distribution.

As shown above, near 100% generation of optical vortices is achieved without polarization control for oblique incidence. It should be noted, however, that the light polarization is in general not conserved upon reflection at oblique incidence. The values shown in Figs. 2(c) and 2(d) are the phase for the p-polarized component of light; although the s-polarized component also shows a similar relationship between the spatial helix phase and the reflected light phase, the exact relationship differs from that of the p-polarized component, and thus a change in polarization occurs. Figure 4 shows the spatial phase dependence of the reflected light polarization at normal and oblique incident angles, where the sign of the ellipticity indicates the handedness of the polarization (positive for RCP and negative for LCP). Although the ellipticity is close to unity for RCP light at normal incidence (the slight reduction is attributed to the anisotropic reflection at the LC-glass interface), smaller values are obtained for oblique incidence, implying that the reflected light is elliptically polarized. LCP also becomes elliptically polarized upon being reflected. Interestingly, LP light is converted into CPs with different rotation senses depending on the polarization angle; $p(s)$-polarized light is reflected as a left(right)-handed elliptically polarized light. These effects are caused by a combination of several effects such as Fresnel reflection at the ChLC-glass interface and difference in the coupling efficiency for p- and s-polarized modes. Because the spatial variation in polarization of an optical vortex affects the field distribution when focused by a lens [25], measures should be taken to avoid detrimental effects, depending on the application. Possible ways to reduce the depolarization effect includes using a ChLC with smaller birefringence or using a thicker device at a smaller incidence angle.

In conclusion, we have theoretically and experimentally demonstrated generation of optical vortices from ChLCs containing a screw dislocation in the spatial distribution of the helix phase. The Bragg-reflection-based conversion mechanism enables high efficiency, polychromatic optical vortex generation without the need of fine-tuning. Even though Bragg reflection of ChLCs is circularly polarization sensitive, incident-polarization-insensitive vortex generation is possible by utilizing the total reflection band that appears at large incidence angles. The device should be useful for generating optical vortices from ultrashort pulsed lasers, which have broad lasing spectra, and in microscopy, where devices with small footprints are required. We note that the relationship between the helix phase and the optical phase at oblique incidence can be used to design devices with other optical functions, such as lensing and deflection. The concept of helix phase control can potentially be applied to other natural and artificial chiral systems, such as the smectic C* and the cholesteric blue phases [26,27], chiral sculptured films [28], and helix metamaterials [29]. Also, geometries different from a flat slab can be used, as optical vortex generation based on the same mechanism has recently been demonstrated using a self-organized ChLC droplet [30].

This work was supported by Grant-in-Aid for JSPS Fellows (No. 15J00288), MEXT Photonics Advanced Research Center (PARC) at Osaka University, and JST PRESTO.

*yoshida@eei.eng.osaka-u.ac.jp

[1] M. R. Dennis, K. O'Holleran, and M. J. Padgett, Prog. Opt. **53**, 293 (2009).
[2] A. M. Yao and M. J. Padgett, Adv. Opt. Photonics **3**, 161 (2011).
[3] J. E. Curtis and D. G. Grier, Phys. Rev. Lett. **90**, 133901 (2003).
[4] L. Paterson, M. P. MacDonald, J. Arlt, W. Sibbett, P. E. Bryant, and K. Dholakia, Science **292**, 912 (2001).
[5] G. Gibson, J. Courtial, M. J. Padgett, M. Vasnetsov, V. Pas'ko, S. M. Barnett, and S. Franke-Arnold, Opt. Express **12**, 5448 (2004).
[6] G. Foo, D. M. Palacios, and G. A. Swartzlander, Opt. Lett. **30**, 3308 (2005).
[7] S. Fürhapter, A. Jesacher, S. Bernet, and M. Ritsch-Marte, Opt. Express **13**, 689 (2005).
[8] M. Beijersbergen, R. Coerwinkel, M. Kristensen, and J. Woerdman, Opt. Commun. **112**, 321 (1994).

[9] J. Arlt, K. Dholakia, L. Allen, and M. J. Padgett, J. Mod. Opt. **45**, 1231 (1998).
[10] B.-y. Wei, W. Hu, Y. Ming, F. Xu, S. Rubin, J.-g. Wang, V. Chigrinov, and Y.-q. Lu, Adv. Mater. **26**, 1590 (2014).
[11] D. Voloschenko and O. D. Lavrentovich, Opt. Lett. **25**, 317 (2000).
[12] L. Marrucci, C. Manzo, and D. Paparo, Phys. Rev. Lett. **96**, 163905 (2006).
[13] S. Slussarenko, A. Murauski, T. Du, V. Chigrinov, L. Marrucci, and E. Santamato, Opt. Express **19**, 4085 (2011).
[14] E. Brasselet, N. Murazawa, H. Misawa, and S. Juodkazis, Phys. Rev. Lett. **103**, 103903 (2009).
[15] Y. Yang, W. Wang, P. Moitra, I. I. Kravchenko, D. P. Briggs, and J. Valentine, Nano Lett. **14**, 1394 (2014).
[16] E. Karimi, S. A. Schulz, I. D. Leon, H. Qassim, J. Upham, and R. W. Boyd, Light Sci. Appl. **3**, e167 (2014).
[17] J. Leach, G. M. Gibson, M. J. Padgett, E. Esposito, G. McConnell, A. J. Wright, and J. M. Girkin, Opt. Express **14**, 5581 (2006).
[18] P. Yeh and C. Gu, *Optics of Liquid Crystal Displays* (John Wiley & Sons, Inc., New York, 2009), 2nd ed., Chap. 7, pp. 461–484.
[19] T. Scharf, *Polarized Light in Liquid Crystals and Polymers* (John Wiley & Sons, Inc., New York, 2006), Chap. 11, pp. 349–391.
[20] J. Kobashi, H. Yoshida, and M. Ozaki, Nat. Photonics **10**, 389 (2016).
[21] V. G. Chigrinov, V. M. Kozenkov, and H.-S. Kwok, *Photoalignment of Liquid Crystalline Materials: Physics and Applications* (Wiley, New York, 2008).
[22] A. V. Carpentier, H. Michinel, J. R. Salgueiro, and D. Olivieri, Am. J. Phys. **76**, 916 (2008).
[23] H. Takezoe, Y. Ouchi, M. Hara, A. Fukuda, and E. Kuze, Jpn. J. Appl. Phys. **22**, 1080 (1983).
[24] D. W. Berreman, J. Opt. Soc. Am. **62**, 502 (1972).
[25] C. J. R. Sheppard, Opt. Express **22**, 18128 (2014).
[26] I. Dierking, Symmetry **6**, 444 (2014).
[27] D. C. Wright and N. D. Mermin, Rev. Mod. Phys. **61**, 385 (1989).
[28] K. Robbie, J. Brett, and A. Lakhtakia, Nature (London) **384**, 616 (1996).
[29] J. K. Gansel, M. Thiel, M. S. Rill, M. Decker, K. Bade, V. Saile, G. von Freymann, S. Linden, and M. Wegener, Science **325**, 1513 (2009).
[30] M. Rafayelyan, G. Tkachenko, and E. Brasselet, preceding Letter, Phys. Rev. Lett. **116**, 253902 (2016).